Results in Engineering 28 (2025) 107278

Contents lists available at ScienceDirect

Results in Engineering

journal homepage: www.sciencedirect.com/journal/results-in-engineering

Research paper

Optimal design of risk-based average charts for autocorrelated measurements

Aamir Saghir [a], Zahid Khan [b], Jean-Claude Malela-Majika [c], Zsolt T. Kosztyán [b,d,*]

[a] Department of Statistics, Mirpur University of Science and Technology (MUST), Mirpur, 10250, AJK, Pakistan
[b] Department of Quantitative Methods, University of Pannonia, Egyetem str.10, Veszprem, 8200, Hungary
[c] Department of Statistics, Faculty of Natural and Agricultural Sciences, University of Pretoria, Hatfield, 0028, Pretoria, South Africa
[d] Institute of Advanced Studies, Koszeg, Charnel str., 14, Koszeg, 9730, Hungary

ARTICLE INFO

Dataset link: https://CRAN.R-project.org/package=rbcc

Keywords:
Autocorrelation
Control charts
Decision error
EWMA
Measurement uncertainty
Optimization
Phase I

ABSTRACT

Control charts are vital for real-time production process monitoring tasks, as they help monitor and maintain consistent product quality and detect variations early. In statistical process control (SPC), the use of risk-based control charts (RBCCs) improves the traditional control chart logic by considering decision risks, which can be influenced by factors such as measurement errors or sampling procedures. The traditional RBCC methodology relies on one of the fundamental assumptions: that process data are statistically independent. However, the characteristics monitored by process management are not always statistically independent of one another. This raises significant concerns for practitioners, as many processes in real-world scenarios generate autocorrelated observations. In this study, the issue of autocorrelation in the commonly used RB average charts ($\bar{X}$ and the exponentially weighted moving average (EWMA)) is addressed by incorporating an autocorrelated structure into the RB design. The proposed approach extends the RB average charts to better account for the autocorrelation problem. To validate the adequacy of the proposed design, Monte Carlo simulations are carried out under different autocorrelation settings. The numerical results indicate that the presence of autocorrelation significantly distorts the performance of existing RB $\bar{X}$ and EWMA designs in terms of the total cost of a decision. In contrast, the overall cost associated with the proposed RB charts is less affected as the autocorrelation factor increases. A real dataset is used to demonstrate the proposed design and its applicability in real-world scenarios.

1. Introduction

All manufacturing operations naturally involve some degree of variability [16]. While not all variability is harmful, excessive or uncontrolled variations due to assignable causes can negatively impact process performance. To achieve increased process performance, practitioners use various methods and tools to reduce this harmful variability and improve the quality of products before they are released for practical use in the field [5]. Among the various developed improvement techniques, statistical process control (SPC), as a component of statistical quality control (SQC), is a widely recognized and practical approach that is often applied for process improvement purposes [33,38,12]. SPC encompasses a range of powerful tools that help industry professionals achieve greater process consistency and minimize variations, ultimately leading to improved quality outcomes [6]. In modern industries, control charts are typically used to check whether process variations are due to random causes or specific harmful causes [52,62,23].

Control charts are typically categorized into memory-based and memoryless types [1]. Shewhart-type charts belong to the memoryless category and are particularly adept at rapidly detecting large process shifts [31]. As an advancement over memoryless control charts, memory-type control charts such as the exponentially weighted moving average (EWMA) chart and the cumulative sum (CUSUM) chart offer improved sensitivity to small shifts owing to the use of both past and current information [7]. Control charts are also commonly used to evaluate the ongoing precision and accuracy of measurement systems over time by identifying deviations from predefined standards [13]. In practice, regardless of which type of control chart is implemented in real-world scenarios, SPC generally operates under the assumption that the data collected from a process are obtained through a perfect mea-

* Corresponding author.
E-mail address: kosztyan.zsolt@gtk.uni-pannon.hu (Z.T. Kosztyán).

https://doi.org/10.1016/j.rineng.2025.107278
Received 30 June 2025; Received in revised form 10 September 2025; Accepted 13 September 2025

Available online 17 September 2025

surement system [37]. The assumption of a perfect measurement system is often unrealistic, as the characteristics of interest may be influenced by numerous elements, including human factors (e.g., recording errors, improper operation, and poor sampling practices), environmental conditions (e.g., humidity, temperature, and pressure), and flaws in the measurement system itself due to factors such as instrument miscalibration and equipment degradation [34].

A measurement error refers to the discrepancy between the actual and recorded values of a characteristic [15]. When measurement uncertainties or errors are present in a system, they contribute to increased observed process variability and may cause adverse effects due to unfavorable outcomes stemming from erroneous judgments and decisions [55]. The statistical performance of control charts decreases as the degree of measurement uncertainty increases despite a fixed process variation level [10]. More precisely, monitoring the variations exhibited by the mean and variance of a characteristic in the presence of significant measurement errors reduces the ability of control charts to detect parameter shifts in the underlying quality characteristic [28]. Overall, measurement uncertainty leads to high false-alarm rates under in-control (IC) conditions, whereas the ability of control charts to detect out-of-control (OC) situations decreases considerably [44]. Although measurement uncertainty has been extensively highlighted in the SPC literature, research on control charts that account for measurement error is still limited and far less prevalent than anticipated [30].

Numerous approaches have been proposed in the literature to optimize the cost or risk associated with system measurement uncertainty (see Jafarian-Namin et al. [18], Shojaee et al. [50]). These approaches are based on statistical design (SD), economic design (ED), or economic-statistical design (ESD) to optimize the cost of a process or perform risk adjustment. The impact of measurement uncertainty was examined in these studies, but they failed to offer a comprehensive solution or suggest alternative control charts for minimizing the chances of obtaining incorrect decisions. A risk-based (RB) strategy is essential in modern SQC, as it accounts for both the probabilities and severity levels of process failure factors that are often missed by traditional methods [24,42]. This approach supports priorities such as safety and compliance, motivating the development of control charts that guide actions on the basis of risk importance. Thus, there is a strong motivation to develop a new family of control charts based on RB principles [26]. As a strategy for managing the risks arising from measurement uncertainty, a family of RB control charts (RBCCs) was designed in Kosztyán and Katona [26] and Katona et al. [22]. In contrast with the Shewhart and ED models, RBCCs incorporate all four possible decision outcomes to minimize the number of incorrect decisions under parameter uncertainty [21]. RBCCs utilize simulation and optimization methods to identify the best chart parameters, minimizing the likelihood of producing incorrect decisions during process monitoring [25]. The results indicate that adopting an RB control scheme significantly decreases the incurred decision costs despite the presence of nonnormal measurement errors.

Traditional SPC methods, including both standard control charts and RBCCs, are typically based on the assumption that process data are statistically independent. However, as highlighted by numerous researchers, this assumption is often violated in real-world scenarios [4,20,2,39,60,19]. Most process data are correlated in many applications, such as chemical, semiconductor, and pharmaceutical manufacturing tasks. In such cases, applying standard control charts designed for independent data can result in a significantly reduced IC average run length (ARL), thereby increasing the likelihood of false alarms and compromising the reliability of the developed monitoring scheme. This effect has been documented by several authors, such as Maragah and Woodall [32], Schmid [48], Stoumbos and Reynolds Jr [54], MacCarthy and Wasusri [29], Psarakis and Papaleonida [40], Schat et al. [47], Tyagi and Yadav [56].

The challenge of managing autocorrelation in control chart designs has recently received significant attention, as many industrial processes naturally produce autocorrelated outcomes. In recent research, numerous authors have developed and modified monitoring schemes for autocorrelated data. For example, Nguyen et al. [36] developed an RZ control chart for monitoring the ratio of two quality characteristics under the assumption of dependent observations. Silpakob et al. [51] suggested a modified EWMA control chart under a correlated data structure. Quintero-Arteaga et al. [41] designed an adaptive synthetic $\bar{x}$ chart for first-order autoregressive data. Sabahno [43] developed an adaptive max-type multivariate control chart under a vector-mixed autoregressive and moving-average autoregressive model. Under profile monitoring schemes with correlated data structures, Yeganeh et al. [60] proposed using machine learning techniques as alternatives to traditional statistical control charts. Sheu et al. [49] investigated the properties of the generally weighted moving average (GWMA) chart for identifying the small process mean shifts of autocorrelated observations. Saha et al. [45] introduced the multivariate run sum (MRS) chart for monitoring autocorrelated processes, employing a first-order vector autoregressive model combined with an s-skip sampling strategy. [58] created and examined an AEWMA control chart by fitting the time series model's residual and determining the best control parameters for autocorrelation processes. Nazari and Sogandi [35] introduced several recognition models that leverage a customized convolutional network in combination with pretrained networks such as VGG19, MobileNet, and LeNet to detect control chart patterns (CCPs) in autocorrelated processes. Jafarian-Namin et al. [19] introduced a robust design framework for processes characterized by imperfections and autocorrelation in the presence of uncertainty.

Thus, misspecified autocorrelation structures and inaccurate cost estimates (measurement uncertainty) can significantly distort decision-making outcomes in various domains where decision makers rely on statistical models, control charts, or predictive analytics. The former can lead to distorted perceptions of risk and system behavior, whereas the latter skews the cost-benefit analysis and risk management strategies. Together, these errors can compound decision-making problems, leading to overreactions, underreactions, inefficient resource allocation, and missed opportunities. To mitigate these risks, it is essential for decision makers to rigorously assess both autocorrelation structures and cost estimates to ensure that decisions are informed by accurate, reliable data. Consequently, developing new methods to minimize the number of incorrect decisions under parameter uncertainty remains a crucial and promising area for further research in the field of SQC.

To the best of the authors' knowledge, the impact of autocorrelation on RBCCs has not been previously examined. This gap is notable, as these charts are widely used and easily implemented via the rbcc R package. Because autocorrelation is common in many industrial processes, enhancing the effectiveness of RBCCs under such conditions is essential. This study addresses that need by investigating (i) how the decision risks arising from both autocorrelation and measurement uncertainty affect the performance of RB average control charts (A_1) and (ii) the effectiveness of RB average charts for use with simulated and actual industrial data (A_2).

The major contributions of this study can be outlined as follows.

- $\mathbf{C}_1$ The RBCC framework is extended to accommodate autocorrelated measurements, enhancing its applicability to current SPC practices.
- $\mathbf{C}_2$ Considering the impact of autocorrelation on decision-making and the associated costs, an optimal design methodology is adopted for the commonly used RB average charts.
- $\mathbf{C}_3$ The effectiveness of the proposed charts is validated using both simulation experiments and real-world examples involving autocorrelated data.

The rest of the paper is organized as follows. RB average control charts are proposed in the presence of measurement errors and autocorrelation in Section 2. The numerical results obtained on the basis of a simulation and a real-world application are reported in Section 3. Sec-

tion 4 concludes the paper with a summary of the key findings. The limitations of this work and future directions are given in Section 5.

2. Methodology

We consider the RB methodology suggested by Kosztyán and Katona [27] when designing the RB autoregressive (i) $\bar{X}$ (a memoryless) and (ii) EWMA $\bar{X}$ (memory-based) control charts. This methodology consists of four steps: (1) computing the parameters of traditional average control charts for autoregressive (AR) processes, (2) performing cost estimation for the decision outcomes, (3) determining the overall cost of the model, and (4) optimizing the control limits for the AR processes examined in Phase I.

2.1. Computation of control limits

2.1.1. Process models for addressing autocorrelation

Assume that $X_{i,j}$, where $i = 1,2,3,\ldots$ and $j = 1,2,3,\ldots,n$ is a sequence of observations derived from a normal distribution with a mean of μ and a variance of σ^2, which are autocorrelated and can be described by an AR(1) process as follows:

$$X_{i,j} = \mu + \phi\left(X_{i,j} - \mu\right) + \epsilon_{i,j}, \tag{1}$$

where $\phi\,(|\phi| < 1)$ is the AR(1) parameter, which describes the level of autocorrelation that is present in the process, and $\epsilon_{i,j} \sim N(0,\sigma_\epsilon^2)$ denotes white noise (independently and identically distributed (i.i.d.) with a constant mean, a constant variance, and an autocorrelation of zero at all i lags), where σ_ϵ represents the standard deviation of the white noise. The mean and variance of the measurement of the process $(X_{i,j})$ are $E(X_i) = \mu$ and $V(X_i) = \sigma^2 = \frac{\sigma_\epsilon^2}{1-\phi^2}$, respectively, for all $i = 1,2,3,\ldots$. Obviously, $V(X_i) = \sigma^2 = \sigma_\epsilon^2$ when $\phi = 0$.

2.1.2. Estimation

In the RB methodology, the first step is to estimate the plotting statistic, its average and standard deviation, and the control limits of the underlying control chart. In this paper, $\bar{X}$ and EWMA $\bar{X}$ charts are considered, and the parameters of these charts can be estimated on the basis of the Phase-I data.

$\bar{X}$ chart

In the case of an $\bar{X}$ chart, the plotting statistic is the ith sample mean. If $X_{i,j}$ is a Phase-I data point following the AR(1) model defined in Eq. (1), then the i^{th} sample mean is computed by Wu [59] as follows:

$$\bar{X}_i = \frac{1}{n}\sum_{j=1}^{n} X_{ij}. \tag{2}$$

The expected value and variance of $\bar{X}_i$ [8] for all $i = 1,2,3,\ldots$ are as follows:

$$E\left(\bar{X}_i\right) = \mu_{\bar{X}} = \mu \tag{3}$$

and

$$Var\left(\bar{X}_i\right) = \sigma_{\bar{X}}^2 = \frac{\sigma_\epsilon^2}{n\left(1-\phi^2\right)}\left[1 + 2\sum_{h=1}^{n-1}\left(1-\frac{h}{n}\right)\phi^h\right], \tag{4}$$

where h denotes the time difference between two observations, and when $\phi = 0$, Eq. (4) yields $\sigma_{\bar{X}}^2 = \frac{\sigma^2}{n}$.

The control limits of the Shewhart-type $\bar{X}$ chart under the AR(1) process can be expressed as follows:

$$UCL_{\bar{X}} = \mu_{\bar{X}} + k_x\sigma_{\bar{X}} \tag{5}$$

and

$$LCL_{\bar{X}} = \mu_{\bar{X}} - k_x\sigma_{\bar{X}}. \tag{6}$$

After substituting the values of $\sigma_{\bar{X}}$ given in Eq. (4), we obtain

$$UCL_{\bar{X}} = \mu_{\bar{X}} + k_x\frac{\sigma_\epsilon}{\sqrt{n\left(1-\phi^2\right)}}\left[1 + 2\sum_{h=1}^{n-1}\left(1-\frac{h}{n}\right)\phi^h\right]^{\frac{1}{2}} \tag{7}$$

and

$$LCL_{\bar{X}} = \mu_{\bar{X}} - k_x\frac{\sigma_\epsilon}{\sqrt{n\left(1-\phi^2\right)}}\left[1 + 2\sum_{h=1}^{n-1}\left(1-\frac{h}{n}\right)\phi^h\right]^{\frac{1}{2}}, \tag{8}$$

where $\mu_{\bar{X}} = \mu$ is the mean of the process (expected value), $\sigma_\epsilon = \sigma$ is the standard deviation of the process, $k_x\sigma$ is the change exhibited by the mean of the process expressed in standard deviation units for a prespecified level of significance (usually, $\alpha = 0.0027$, and $k_x = 3$ [33]), and $UCL_{\bar{X}}$ and $LCL_{\bar{X}}$ denote the upper and lower control limits, respectively. The process parameters in applications are typically unknown and are calculated via preliminary samples (Phase I) under the assumption of an IC process. On the basis of these data, the average μ is estimated as follows:

$$\bar{\bar{X}} = \frac{1}{m}\sum_{i=1}^{m}\bar{X}_i = \frac{1}{m}\sum_{i=1}^{m}\left(\frac{1}{n}\sum_{j=1}^{n}X_{ij}\right), \tag{9}$$

and the standard deviation of the process σ is determined by

$$\bar{s} = \left(\frac{1}{m-1}\sum_{i=1}^{m}(\bar{X}_i - \bar{\bar{X}})^2\right)^{\frac{1}{2}}, \tag{10}$$

where $\bar{s}$ is a biased estimate; to obtain an unbiased estimate of the true σ, $\bar{s}$ is divided by c_4 [33]. In the phase I analysis, the bias correction factor c_4 depends on the subgroup size and sample size and is defined as follows:

$$c_4 = \sqrt{\frac{2}{m(n-1)}}\frac{\gamma(\frac{m(n-1)+1}{2})}{\gamma(\frac{m(n-1)}{2})},$$

where $\gamma(.)$ denotes a gamma function. Therefore, the control limits of the Shewhart $\bar{X}$ chart under the AR(1) process and parameter estimation are as follows:

$$UCL_{\bar{X}} = \bar{\bar{X}} + \frac{k_x\bar{s}}{c_4\sqrt{n\left(1-\phi^2\right)}}\left[1 + 2\sum_{h=1}^{n-1}\left(1-\frac{h}{n}\right)\phi^h\right]^{\frac{1}{2}} \tag{11}$$

$$LCL_{\bar{X}} = \bar{\bar{X}} - \frac{k_x\bar{s}}{c_4\sqrt{n\left(1-\phi^2\right)}}\left[1 + 2\sum_{h=1}^{n-1}\left(1-\frac{h}{n}\right)\phi^h\right]^{\frac{1}{2}} \tag{12}$$

EWMA chart

To apply the EWMA chart to the autocorrelated observations $(X_{i,j})$, the exponentially smoothed moving average statistic is determined as follows [17,9]:

$$Z_i = \lambda\bar{X}_i + (1-\lambda)Z_{i-1}, \tag{13}$$

where Z_i is the sample statistic for sample i, $\lambda, 0 < \lambda \le 1$ is the smoothing parameter, and $Z_0 = \mu$. The control limits for the EWMA chart under the AR(1) process are defined as follows:

$$UCL_{EWMA} = \mu_{\bar{X}} + k_{ex}\sigma_{\bar{X}}\sqrt{\left(\frac{\lambda}{2-\lambda}\right)} \tag{14}$$

and

$$LCL_{EWMA} = \mu_{\bar{X}} - k_{ex}\sigma_{\bar{X}}\sqrt{\left(\frac{\lambda}{2-\lambda}\right)}. \tag{15}$$

Similarly, substituting the value of $\sigma_{\bar{X}}$ yields the following:

Table 1
Decision results that can be derived from SPC (from Kosztyán et al. [25]).

	Noticed attribute	
Actual attribute	In-control	Out-of-control
In-control	c_{11}	c_{10}
Out-of-control	c_{01}	c_{00}

$$UCL_{EWMA} = \mu_{\bar{X}} + k_{ex}\frac{\sigma_\epsilon}{\sqrt{n\left(1-\phi^2\right)}}\left[1+2\sum_{h=1}^{n-1}\left(1-\frac{h}{n}\right)\phi^h\right]^{\frac{1}{2}} \times\sqrt{\left(\frac{\lambda}{2-\lambda}\right)} \tag{16}$$

and

$$LCL_{EWMA} = \mu_{\bar{X}} - k_{ex}\frac{\sigma_\epsilon}{\sqrt{n\left(1-\phi^2\right)}}\left[1+2\sum_{h=1}^{n-1}\left(1-\frac{h}{n}\right)\phi^h\right]^{\frac{1}{2}} \times\sqrt{\left(\frac{\lambda}{2-\lambda}\right)}, \tag{17}$$

where k_{ex} is the control charting constant in the case of an EWMA chart. Note that when $\phi = 0$ (uncorrelated data), the control limits defined in Eq. (14) and Eq. (15) coincide with the traditional EWMA control chart limits given in Katona et al. [22] and Saleh et al. [46]. When $\lambda = 1$, the EWMA chart decreases to the Shewhart-type $\bar{X}$ chart under the AR(1) model [61]. In the case of parameter estimation, the process mean ($\mu_{\bar{X}}$) is replaced by a sample estimate $\bar{\bar{X}}$, and the standard deviation (σ_ϵ) is replaced by $\bar{s}/c_4$, as shown in Eq. (9) and Eq. (10), respectively.

2.2. Decision outcomes and cost estimation

Measurement uncertainty is assumed to be present in the target system in the RB methodology. As a result, the measurement error (e) distorts the real characteristic value of the examined product (x), and each observed value (y) can be written as follows by assuming a simple linear error model ([3]):

$$Y_{i,j} = X_{i,j} + e_{i,j}, \tag{18}$$

where $X_{i,j}$ represents the actual realization of the process (without measurement error) following the AR(1) model defined in Eq. (1), $e_{i,j}$ represents the measurement error with respect to the quality characteristics due to system uncertainty and $Y_{i,j}$ denotes the observed quality characteristics of a production process (with measurement error) under the AR(1) model. The measurement error ($e_{i,j}$) is independent of the white noise term ($\epsilon_{i,j}$).

When measurement error is present in the system, four distinct decision outcomes can be obtained because the observed attributes (y) are distorted from the real qualities (x). These decisions are (1) correct acceptance, (2) type I error, (3) type II error and (4) correct control. The possible outcomes on the basis of observable and real product attributes are shown in Table 1.

In Table 1, the costs of proper acceptances are denoted by c_{11}, those of type I errors (false controls) are represented by c_{10}, those of type II errors (false acceptances) are defined as c_{01}, and those of correct controls when an OOC state is correctly diagnosed are c_{00}.

By examining the cost components retrieved from the enterprise resource planning (ERP) system of the examined manufacturer, the price of each choice can be ascertained. For a complete explanation of the cost estimation step of the decision-making process, the reader can consult [26], which outlines the key elements and offers a real-world illustration of the estimation method.

2.3. Overall cost of the process

Third, the overall cost of the monitoring process based on these four decisions must be estimated via the RB methodology [27]. The benefit of the RB approach is that unlike the ED of control charts [57], all four states are considered in terms of the total cost of the process: allowing the regulated process to continue, looking for assignable causes when the process deviates from control, and identifying the two types of decision errors (type I and type II). According to Kosztyán and Katona [26], by adding the costs of each decision result, the overall decision cost can be estimated as follows:

$$\begin{aligned} TC &= C_{11} + C_{10} + C_{01} + C_{00} \\ &= q_{11}c_{11} + q_{10}c_{10} + q_{01}c_{01} + q_{00}c_{00}, \end{aligned} \tag{19}$$

where C_{ab} represents the total cost associated with a particular decision outcome, q_{ab} indicates the number of instances (cases) that occur during the control scheme, and c_{ab} denotes the cost of each decision estimated or assessed by the ERP system (see Katona et al. [22]). The sample means (X_i and Y_i) are compared to the control limits that are established by considering the distorted processes caused by measurement errors for identifying type I and type II errors. The cost of the sample mean statistic of the decision outcome is computed.

2.4. Optimal control limits

The final step in the RB methodology is to optimize the control limits. Let K be a one-dimensional vector of the optimal control limit constants of the proposed RB $\bar{X}$ and RBEWMA $\bar{X}$ charts (i.e., $K = (k_x^*, k_{ex}^*)$). To find the optimized control limits of the proposed charts under the AR(1) model, the total cost of the decisions (TC) defined in Eq. (19) is minimized for the control charting constants k_x^* and k_{ex}^*. The optimization problem is stated as follows:

$$\begin{aligned} &\underset{\mathbf{k_s}}{\text{minimize}} \quad TC(\mathbf{k_s}) \\ &\text{subject to} \quad \mathbf{k_s} > 0 \end{aligned} \tag{20}$$

where k_s is the sth element of the vector K. Eq. (20) is a straightforward optimization problem that can be resolved using any optimization technique. The TC function does not have a closed-form expression or an analytical gradient; therefore, the Nelder-Mead approach is well suited for such black-box functions because it does not require derivatives. We also use the Nelder-Mead algorithm in this paper to optimize the TC. In this study, only the control limits are optimized; however, as demonstrated in Kosztyán and Katona [27], this approach can be paired with the best sample size and sampling interval settings, as performed for the ED.

RBCCs are designed to minimize the total expected cost or loss, not to satisfy a fixed ARL criterion such as ARL = 370. The ARL is a statistical metric, not an economic metric, that ignores the real-world cost differences between false alarms and missed detections [53]. Thus, using the optimal solution of Eq. (20), the optimal control limits of the RB $\bar{X}$ chart for the AR(1) model are obtained as follows:

$$UCL_{RBAR_{\bar{X}}} = \mu_{\bar{X}} + k_x^*\sigma_{\bar{X}} \tag{21}$$

and

$$LCL_{RBAR_{\bar{X}}} = \mu_{\bar{X}} - k_x^*\sigma_{\bar{X}}. \tag{22}$$

The optimal limits of the RBEWMA $\bar{X}$ chart under the AR(1) model are as follows:

$$UCL_{RBAR_{EWMA}} = \mu_{\bar{X}} + k_{ex}^*\sigma_{\bar{X}}\sqrt{\left(\frac{\lambda}{2-\lambda}\right)} \tag{23}$$

and

$$LCL_{RBAR_{EWMA}} = \mu_{\bar{X}} - k_{ex}^*\sigma_{\bar{X}}\sqrt{\left(\frac{\lambda}{2-\lambda}\right)}, \tag{24}$$

where k_x^* or k_{ex}^* is an optimal constant, i.e., a solution of Eq. (20), for a given sample size (n), an observable process distribution, an amount of autocorrelation (ϕ), a measurement uncertainty level ($e_{i,j}$), and decision outcome costs (c_{ab}). In the case of unknown parameters, the parameters are replaced with their respective sample estimates defined in Eq. (9) and Eq. (10), respectively.

Eqs. (21)-(22)) and (23)-(24)) are optimal control limits that reduce the overall loss caused by these decisions while striking a balance between type I and type II errors and providing the traditional counterpart when $k_s = 3, s = 1, 2$. Additionally, these optimal control limits are equal to the control limits of the RB $\bar{X}$ and RBEWMA $\bar{X}$ charts proposed by Katona et al. [22] when $\phi = 0$.

The application of the RBAR model, in which each value depends on its preceding value with the incorporation of a risk component, necessitates a systematic approach, particularly in industrial contexts. The following steps are recommended for practitioners to ensure effective implementation:

- **Data Collection**: Gather historical industrial data, both with and without measurement error, including both actual and observed values. This step is critical for distinguishing between true process behavior and observed discrepancies due to errors in measurement.
- **Parameter Estimation:** Implement the AR(1) model, as defined in Eq. (1), and estimate the model parameters using the actual data (denoted by $X_{i,j}$) that is free from measurement errors. This step provides the foundation for accurate modeling.
- **Control Limit Construction:** The actual, error-free data are used to construct control limits that guide decision-making and process monitoring. These limits are essential for detecting deviations from expected performance.
- **Comparison with Observed Realizations:** Compare the actual process realizations and the observed realizations (which include measurement errors) against the constructed control limits. This comparison allows for the identification of discrepancies or abnormal behavior in the process.
- **Cost Calculation:** Calculate the overall cost associated with the process decisions, factoring in both risk and operational costs. This step helps quantify the economic impact of any deviations from the expected process outcomes.
- **Optimization of Control Limits:** Finally, the control limit constant (k_s) is adjusted to minimize the total decision-making cost of the process, as expressed in Eq. (20). Fine-tuning this constant ensures that the process remains within optimal operational thresholds while minimizing cost.

By following these steps, practitioners can apply the RBAR model effectively to monitor, control, and optimize industrial processes in the presence of uncertainty and risk.

3. Numerical results

The applicability of the RB $\bar{X}$ and RBEWMA $\bar{X}$ charts under the AR model is statistically examined in this section. The applicability of the proposal is examined under two distinct circumstances. First, a study using a Monte Carlo simulation is conducted in subsection (A) to determine the ideal correction constant of the RB average charts under the AR(1) model. Second, in subsection (B), the optimal parameters for the RB $\bar{X}$ and RBEWMA $\bar{X}$ charts under the AR(1) model are found using an actual dataset involving a master brake cylinder [21].

3.1. Simulation study

Simulation studies are often conducted to validate a new method or scheme and assess its performance under realistic, controlled conditions before it is implemented in real-world processes. We carried out a simulation analysis to validate the applicability of the proposed charts.

Table 2
Input parameters for the simulation analysis.

Sign	Definition	Value
μ_x	Process average	10
σ_x	Process dispersion	0.5
σ_e	Standard deviation of the measurement error	0.05
ϕ	Autocorrelation coefficient	0.1(0.1)0.5,0.8
m	Phase-I data size	1000
n	Sample size	1
r	Number of repetitions of each chart	100
c_{11}	Cost of a correct acceptance	1
c_{10}	Cost of an incorrect control	5
c_{01}	Cost of an incorrect acceptance	60
c_{00}	Cost of a correct control	5
λ	Smoothing parameter	0.20

The simulation study started by generating random numbers ($m = 1000$) for a given sample size, where these samples followed a normal distribution with a mean of μ_x, a standard deviation of σ_x and a correlation of ϕ, as described by the model of Eq. (1). Next, a separate measurement error vector was integrated into the process, with the errors following a normal distribution characterized by an expected value of μ_e and a standard deviation of σ_e. The average RB charts were then designed on the basis of the generated data, and the control limits were optimized to minimize the total decision cost. This strategy, which included developing a process with correlated measurements and measurement errors, performing chart design, and conducting optimization, was iterated 100 times, and the average results were reported. The process for computing the optimal chart constant, evaluating the total cost, and deriving decision outcomes for the RB chart is detailed in Algorithm 1. Table 2 summarizes the input parameters that were used in the

Algorithm 1 Pseudocode for the RB chart with cost optimization.

1: **Input:** obs, n, ϕ, μ_X, va_X, sk_X, ku_X, μ_e, va_e, C, confidence_level, bounds $[LKL, UKL]$
2: Generate true process data $X \leftarrow$`generate_ar1(obs, `ϕ`, `μ_X`, `va_X`, `sk_X`, `ku_X`)`
3: Generate measurement error data $UC \leftarrow$ `data_gen(obs, `μ_e`, `va_e`, 0, 3)`
4: Define a cost function $f(K) \leftarrow$ total cost from `rbcc1(X, UC, C, n, `ϕ`, confidence_level, K)`
5: Optimize K^* by minimizing $f(K)$ over $[LKL, UKL]$ using numerical optimization
6: Evaluate the RBCC result $H \leftarrow$ `rbcc1(X, UC, C, n, `ϕ`, confidence_level, `K^*`)`
7: Add the optimal K^* to the result: $H.par \leftarrow K^*$
8: **Output:** Optimal K^*, total cost (C_0), decision outcomes (P_1 to P_4), control limits (T_1 to T_4), $xbar$, $ybar$

simulation analysis. The simulation was conducted using the same cost structure as that given in Katona et al. [22]. Three designs were considered in this simulation study: (i) the Shewhart $\bar{X}$ chart and the EWMA $\bar{X}$ chart for the AR(1) process without measurement error, which we refer to as 'O'; (ii) the RB $\bar{X}$ and RB EWMA $\bar{X}$ charts that were proposed by Katona et al. [22] with measurement errors and $\phi = 0$, which are named 'RB'; and (iii) the proposed RB $\bar{X}$ and RBEWMA $\bar{X}$ charts with measurement errors under AR(1), which we refer to as 'RBAR'.

The distribution behaviors of TC (the total decision cost) based on the three designs are visualized with box plot diagrams in Figs. 1-2 for the $\bar{X}$ chart and in Figs. 3-4 for the EWMA $\bar{X}$ chart. The distributions and medians of the overall decision cost values calculated for the processes produced by the three designs (O, RB, and RBAR) are shown on the vertical axes in Figs. 1(a)-(b).

Figs. 1-4 demonstrate that the suggested optimization scheme reduced the overall decision costs incurred by the "RBAR" method under different values of ϕ. The "RB" charts performed worse in terms of their total decision costs when correlated attributes were present since inde-

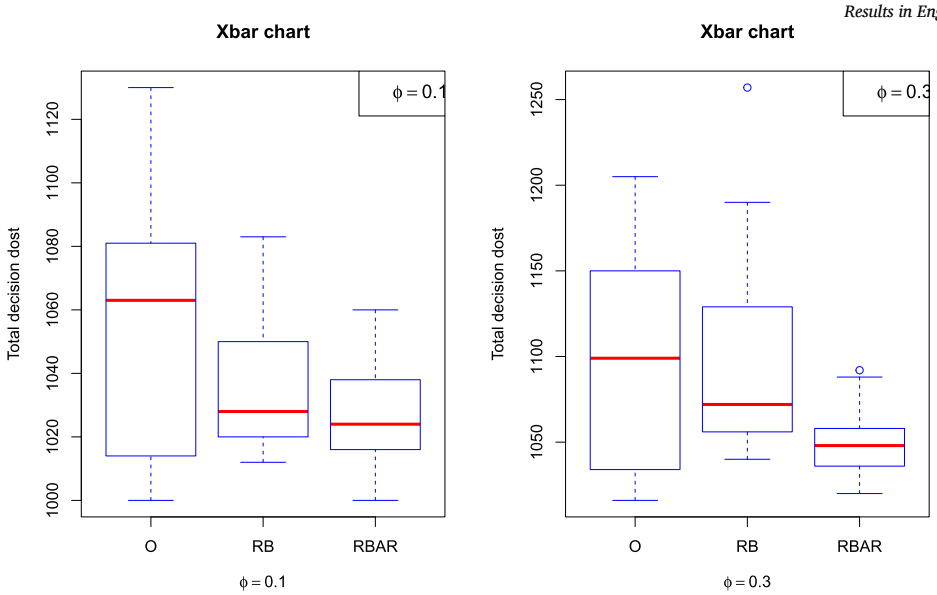

Fig. 1. Distribution of the behavior of the overall decision cost for the $\bar{X}$ chart at $\phi = 0.1$ and 0.3.

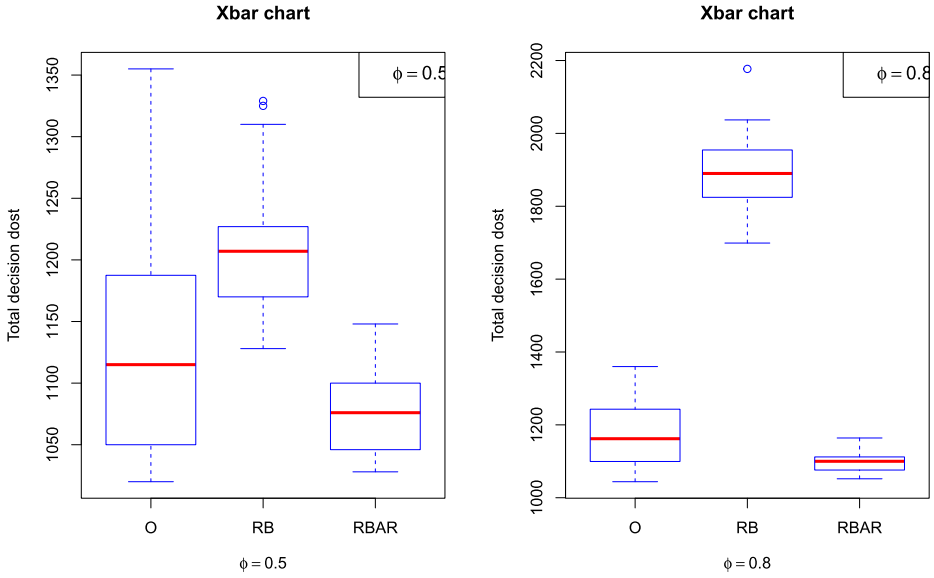

Fig. 2. Distribution of the behavior of the overall decision cost for the $\bar{X}$ chart at $\phi = 0.5$ and 0.8.

pendence among the measurements, particularly a higher value of ϕ, was assumed.

Table 3 displays the parameters of the $\bar{X}$ chart, while the parameters of the EWMA $\bar{X}$ chart are reported in Table 4 using three charts without optimization ("O") and with optimization ("RB" and "RBAR").

Tables 3-4 show that after performing optimization, the chart coefficients decreased for both the "RB" and "RBAR" charts. By balancing the type I and type II errors and given the substantially higher cost of type II errors, the optimization scheme narrowed the control limits to minimize the number of incorrect acceptances. The "RBAR" approach yielded the lowest charting coefficient values among the three tested schemes, especially for large values of ϕ. Consequently, the proposed method expanded the control region to minimize the occurrence of type I errors for each type of RB chart. When $\phi = 0$, "RB" and "RBAR" had the same coefficient values for both average charts.

Furthermore, the total cost of the decision-making step and the cost of each outcome of the decision associated with the $\bar{X}$ and EWMA $\bar{X}$ charts were calculated and are given in Tables 5 and 6, respectively.

The results displayed in Tables 5-6 are as follows.

- When $\phi = 0$, the 'RB' designs of the $\bar{X}$ and EWMA $\bar{X}$ charts, as proposed by [22], are special cases of the proposed 'RBAR' design.
- Although built under the assumption of independent measurements, the "RB" design chart lowered the total cost of the process under smaller autocorrelation values ($0 < \phi \leq 0.3$) than those of the Shewhart-type "O" scheme, which was designed for the AR(1) process. The explanation for these findings suggests that the cost of the decision outcomes produced by the designs of the $\bar{X}$ and EWMA $\bar{X}$ charts is more significant than that incurred when smaller autocorrelation is considered.
- When $\phi > 0.3$, the TC performance of the 'RB' chart was worse than that of the other two competitors. This is because the decisions made by the "RB" average charts were strongly influenced by the assumption of independent measurements and the existence of correlations in the observations.

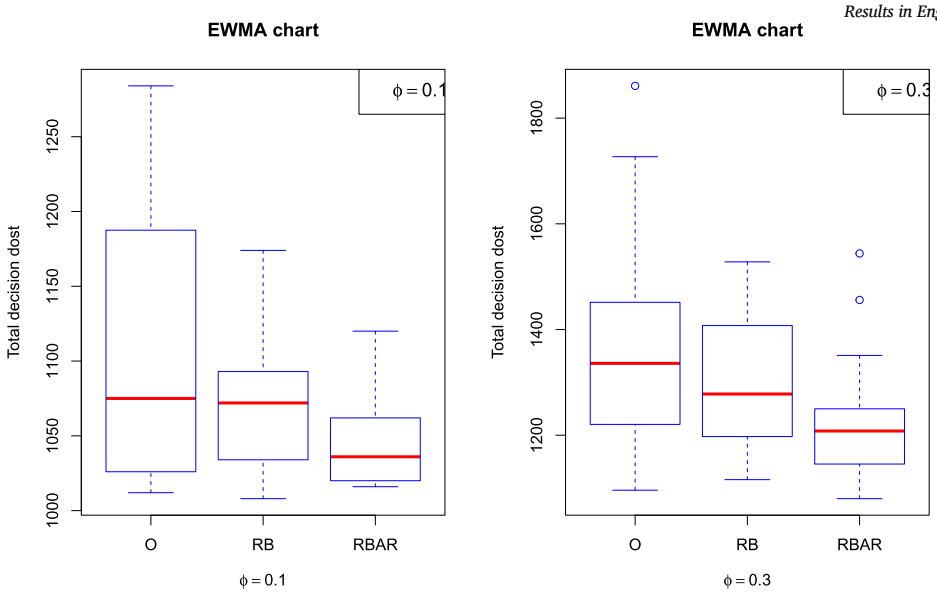

Fig. 3. Distribution of the behavior of the overall decision cost for the EWMA chart at $\phi = 0.1$ and 0.3.

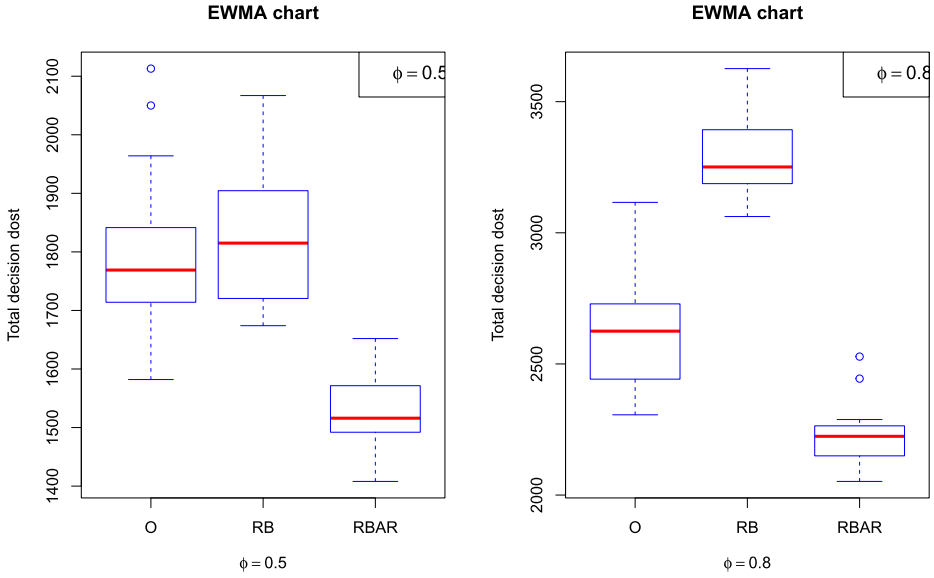

Fig. 4. Distribution of the behavior of the overall decision cost for the EWMA chart at $\phi = 0.5$ and 0.8.

- When $\phi > 0.3$, the "O" design scheme reduced TC more effectively than the "RB" method did because it considers autocorrelation in its design structure.
- The performance of the "RB" charts was significantly affected by a larger autocorrelation value ($\phi > 0.3$). This is because the 'RB' chart is based on the assumption of independence.
- Among the three charts, the proposed 'RBAR" designs for the $\bar{X}$ and EWMA $\bar{X}$ charts performed better in terms of reducing TC for all values of $0 < \phi < 1$.

Cost sensitivity

Furthermore, the design of the RBAR is also significantly influenced by its cost structure, as the RB strategy aims to balance the risks of inducing type I and type II errors during the optimization step. To explore this balance, a sensitivity analysis was conducted on the relative cost of incorrect acceptances versus incorrect rejections (i.e., $c_{01} = (20, 40, 60, 80, 100, 120) * c_{10}$) while keeping the other decision-related costs and input parameters constant in the simulation. This analysis is important because the consequences of a type II error are generally more severe than those of type I error. The results are visualized in Fig. 5 for the RB $\bar{X}$ chart and in Fig. 6 for the RBEWMA $\bar{X}$ chart when $\phi = 0.4$.

As shown in Figs. 5-6, the control charting constant decreased as the cost of incorrect acceptances increased to minimize the total decision cost, and the range of the optimal value of k_s was $(2.75, 3.00)$. As a result, the control region became narrower, implying that stricter control is needed if a missed intervention is more likely. A similar trend was observed for other values of ϕ. The cost of missed interventions has a significant effect on the effectiveness of the RB average charts.

Overall, the 'RBAR' design is more applicable and practical than the existing methods are, and it may be utilized for both independent and dependent measurements when measurement uncertainty is inherent in the target system. Following optimization, the 'RBAR' design reduced the number of type I errors, the number of type II errors, and the total cost of the process under the autoregressive model. Overall cost reduction can be achieved when the cost of a type II error is greater; however, this necessitates a stricter control policy.

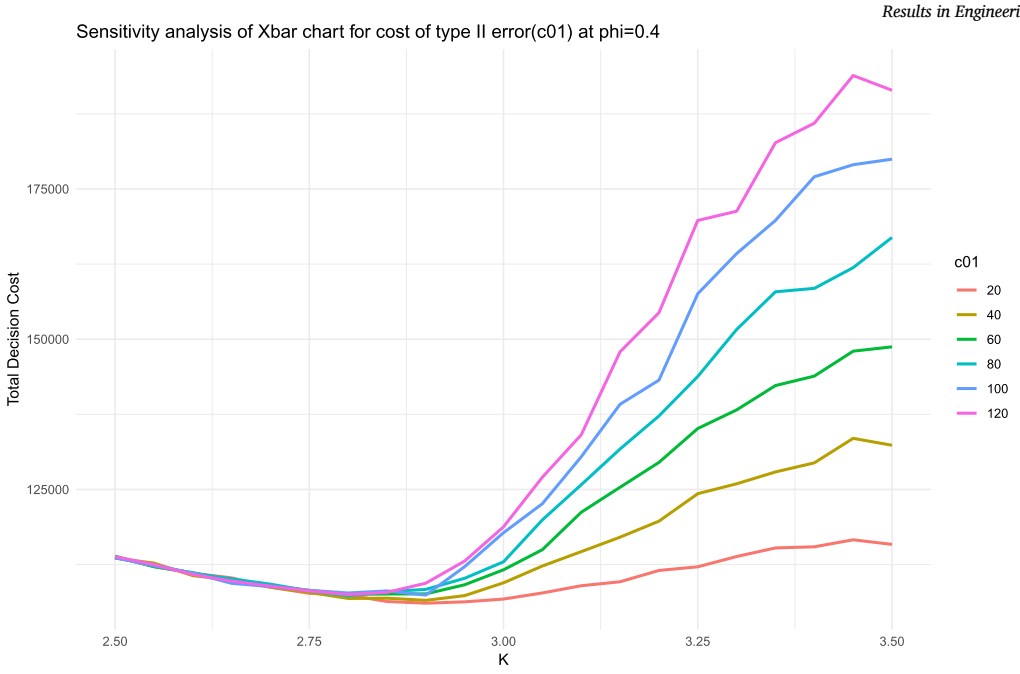

Fig. 5. Sensitivity analysis of the cost of an incorrect acceptance by the RB average chart when $\phi = 0.4$ and n = 1.

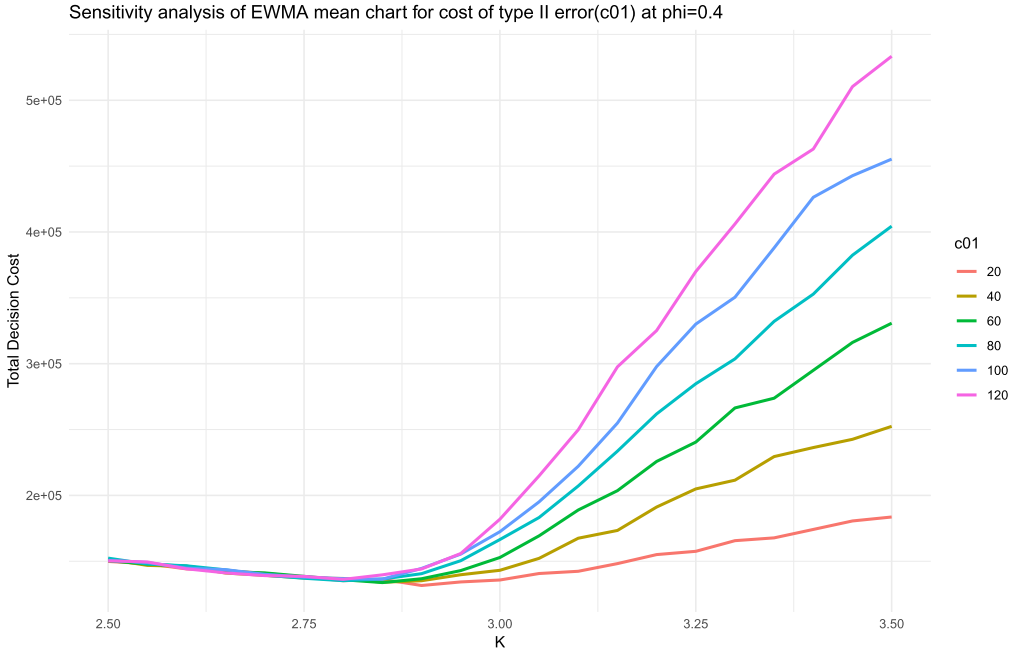

Fig. 6. Sensitivity analysis of the cost of an incorrect acceptance by the RBREMA average chart when $\phi = 0.4, \lambda = 0.2$ and n = 1.

3.2. Data study

The proposed RB charts were further evaluated on a real dataset created by Katona [21]. The dataset consists of fifty brake cylinder cutting length measurements. Each item was measured twice, i.e., once a manual height gauge (the standard manufacturing tool) was used and again with a high-precision 3D instrument, representing the "observed" and "true" product characteristics, respectively. The 50 measurements were recorded with 1 product each time. The 'true' values (indicated as x) signify the accurate measurement of the cutting length via a 3D optical scanner, whereas the 'measured' value (denoted as y) is derived via a manual height gauge (caliper). Following the values of x and y, the measurement error was also calculated with the simple additive model given in Eq. (18) for each i^{th} measurement. Because the dataset was small, a sample size of $n = 1$ was used for this analysis. The estimated cost structure was $C = (1, 20, 160, 5)$, as reported in Katona [21].

First, the independence assumption between these 50 measurements was tested. The amount of autocorrelation was measured on the basis of these 50 observations for various lags (1 to 20). The autocorrelation function (ACF) and partial ACF (PACF) are typically used in time series analysis tasks to understand the autocorrelation structure of a time series and to assist with building models such as the autoregressive integrated moving average (ARIMA) [8]. The ACF and PACF plots produced for the brake cylinder cutting length data are shown in Fig. 7. The black

Table 3
Control limits and coefficients of the $\bar{X}$ chart in the simulation.

ϕ	Type	$\overline{UCL}$	$\overline{LCL}$	$\overline{CL}$	coeff.
0	O	11.50	8.50	10	3.00
	RBAR	11.46	8.54	10	2.91
0.1	O	11.44	8.56	10	3.00
	RB	11.39	8.61	10	2.91
	RBAR	11.40	8.59	10	2.92
0.2	O	11.40	8.60	10	3.00
	RB	11.33	8.67	10	2.91
	RBAR	11.37	8.64	10	2.90
0.3	O	11.38	8.62	10	3.00
	RB	11.28	8.72	10	2.91
	RBAR	11.34	8.67	10	2.89
0.4	O	11.39	8.62	10	3.00
	RB	11.24	8.77	10	2.91
	RBAR	11.35	8.66	10	2.88
0.5	O	11.42	8.58	10	3.00
	RB	11.19	8.81	10	2.91
	RBAR	11.38	8.63	10	2.88
0.8	O	11.88	8.14	10	3.00
	RB	11.10	8.92	10	2.91
	RBAR	11.82	8.20	10	2.87

O: the original control chart for the AR(1) model with no measurement error; RB: the original risk-based control chart with measurement error for $\phi = 0$; and RBAR: the proposed risk-based control chart with measurement error for AR(1) model.

Table 4
Control limits and coefficients of the EWMA chart in the simulation.

ϕ	Type	$\overline{UCL}$	$\overline{LCL}$	$\overline{CL}$	coeff.
0	O	10.30	9.70	10	3.00
	RBAR	10.29	9.71	10	2.89
0.1	O	10.29	9.71	10	3.00
	RB	10.28	9.72	10	2.89
	RBAR	10.28	9.72	10	2.90
0.2	O	10.28	9.72	10	3.00
	RB	10.26	9.77	10	2.89
	RBAR	10.27	9.73	10	2.88
0.3	O	10.28	9.73	10	3.00
	RB	10.32	9.68	10	2.89
	RBAR	10.27	9.74	10	2.84
0.4	O	10.28	9.73	10	3.00
	RB	10.25	9.76	10	2.89
	RBAR	10.27	9.74	10	2.83
0.5	O	10.29	9.72	10	3.00
	RB	10.24	9.76	10	2.89
	RBAR	10.28	9.73	10	2.85
0.8	O	10.38	9.64	10	3.00
	RB	10.24	9.79	10	2.89
	RBAR	10.37	9.65	10	2.86

O: the original control chart for the AR(1) model with no measurement error; RB: the original risk-based control chart with measurement error for $\phi = 0$; and the RBAR: proposed risk-based control chart with measurement error for the AR(1) model.

Table 5
Simulation-based decision counts and overall costs of the $\bar{X}$ chart.

Chart	Type	q_{11}	q_{10}	q_{01}	q_{00}	TC
0	O	996.88	2.10	16.80	12.12	1027.88
	RBAR	995.90	7	0	13.50	1016.40
0.1	O	995.21	2.90	25.80	18.91	1042.81
	RB	993.88	8.45	6	21.45	1029.98
	RBAR	993.87	9.60	0	21.05	1024.52
0.2	O	992.98	5.45	30.60	27.11	1056.13
	RB	990.34	12.45	12	34.85	1049.64
	RBAR	991.86	11.05	0	29.65	1032.56
0.3	O	990.63	4.85	49.21	37.90	1082.58
	RB	984.60	18.65	18.60	56.80	1078.65
	RBAR	988.74	14.31	0	42	1045.04
0.4	O	988.26	4.65	69	48.30	1110.21
	RB	975.13	25.20	38.40	95.95	1134.68
	RBAR	985.58	18.05	1.20	53.95	1058.78
0.5	O	985.16	5.95	88.8	60.85	1140.76
	RB	961.40	28.51	78.6	157.95	1226.45
	RBAR	982.32	20.15	2 50	68.10	1077.99
0.8	O	975.45	5.21	129.60	106.75	1217.00
	RB	807.20	88.85	170.40	860.95	1927.40
	RBAR	970.54	29.75	1.81	117.40	1119.49

O: the original control chart for the AR(1) model with no measurement error; RB: the original risk-based control chart with measurement error for $\phi = 0$; and RBAR: the proposed risk-based control chart with measurement error for the AR(1) model.

Table 6
Simulation-based decision counts and overall costs of the EWMA $\bar{X}$ chart.

Chart	Type	q_{11}	q_{10}	q_{01}	q_{00}	TC
0	O	997.32	2	13.21	10.30	1022.82
	RBAR	996.32	7	0	11.40	1014.72
0.1	O	991.58	5.75	48.60	32.30	1078.23
	RB	989.39	14.55	15.60	37.20	1056.74
	RBAR	989.39	16.70	2.40	36.15	1044.64
0.2	O	979.67	10	81.60	84.85	1156.12
	RB	974.15	25.35	25.80	101.75	1127.05
	RBAR	976.09	27.90	3	91.40	1098.39
0.3	O	960.93	10.05	193.80	169.15	1333.93
	RB	944.60	45.05	60	226.95	1276.60
	RBAR	952.64	51.50	4.80	184.90	1193.84
0.4	O	931.53	16.40	276.60	302.90	1527.43
	RB	896.61	61.70	106.80	466.35	1531.46
	RBAR	919.73	75.40	6.60	325.40	1327.13
0.5	O	891.74	22.41	381.60	487.11	1782.84
	RB	825.71	77.10	139.80	782.70	1825.31
	RBAR	879.65	82.85	10.20	518.05	1490.75
0.8	O	713.44	15.30	451.80	1379.85	2560.39
	RB	463.98	73.05	174.60	2592.50	3304.13
	RBAR	699.07	87.15	7.80	1416.85	2210.87

O: the original control chart for the AR(1) model with no measurement error; RB: the original risk-based control chart with measurement error for $\phi = 0$; and RBAR: the proposed risk-based control chart with measurement error for the AR(1) model.

lines illustrate the ACF and PACF coefficient values of the series at different lags, whereas the blue dashed lines indicate the 95% confidence interval ranges for the ACF and PACF coefficients. The presence of autocorrelation in the cutting length measurements is shown in Fig. 7.

The autocorrelation coefficient of the master brake cylinder data was $\phi = 0.178$ at a lag of 1. The commonly used autocorrelation test, the Durbin–Watson test [11], was applied to statistically test for the pres-

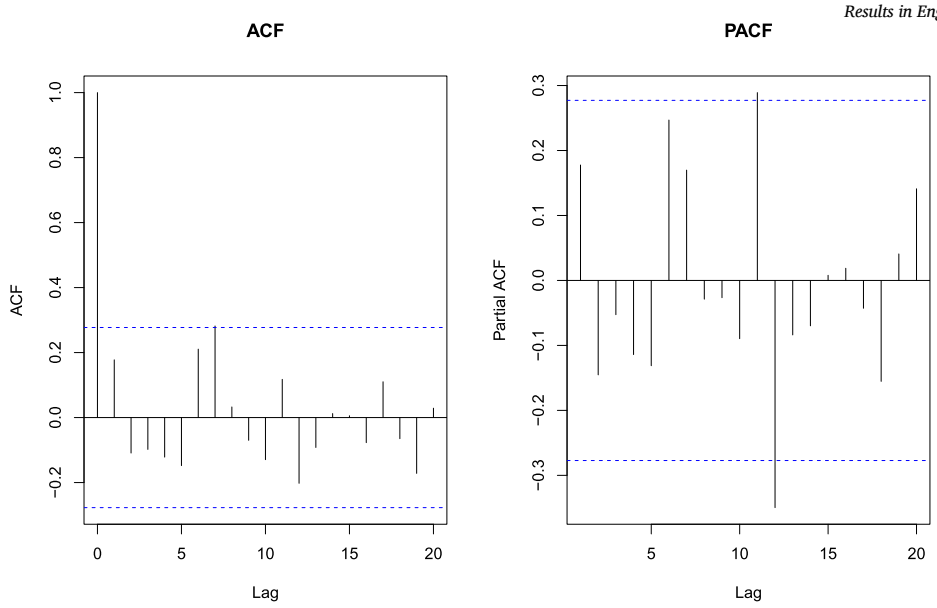

Fig. 7. Autocorrelation and partial autocorrelation function values produced with max.lags = 20 for a practical dataset.

Table 7
Results of a Durbin-Watson test for autocorrelation among the brake cylinder measurements at lag = 1.

Test Type	Data	Statistic	p-value
Durbin Watson	Linear Model X	1.5919	0.0712

Table 8
Control charts based on different schemes for a practical dataset.

Chart	Type	n	ϕ	UCL	LCL	CL	λ	coeff.
X	O	1	0.178	84.78	84.29	84.54	-	3.00
	RB	1	0.178	84.73	84.26	84.54	-	3.56
	RBAR	1	0.178	84.82	84.25	84.54	-	3.42
EWMA	O	1	0.178	84.61	84.45	84.54	0.2	3.00
	RB	1	0.178	84.62	84.45	84.54	0.2	3.12
	RBAR	1	0.178	84.62	84.45	84.54	0.2	3.06

O: the original control chart for the AR(1) model; RB: the original risk-based control chart for independent measurements; and RBAR: the proposed risk-based control chart for the AR(1) model.

ence of autocorrelation in the given data. The results of the DW test are presented in Table 7. The p value indicates that the presence of autocorrelation can be considered at the 10% level of significance or above. The value of DW was less than 2, indicating the existence of a positive autocorrelation in the series [14]. To implement the proposed scheme on the given data, we assumed the existence of autocorrelation and used the AR(1) model for monitoring the cutting length of the brake cylinder process.

Table 8 shows the applied $\bar{X}$ and EWMA $\bar{X}$ control charts based on the Shewhart (O) approach, the [22] RB approach, and the proposed RB autoregressive (RBAR) approach before and after the optimization process is implemented.

Table 8 shows that the control coefficients increased after the optimization of the RB and RBAR approaches was performed on these real data. As discussed by [22], a measurement gauge typically overestimates the actual characteristics of products, resulting in type I errors. The RB and RBAR charts increased the coefficient and relaxed the control region to minimize the number of type I errors. The decision results and total decision costs determined on the cutting length dataset are shown in Table 9.

Table 9
Decision results and overall costs determined for a practical dataset.

Chart	Type	q_{11}	q_{10}	q_{01}	q_{00}	TC
X	O	49	1	0	0	69
	RB	49	1	0	0	69
	RBAR	50	0	0	0	50
EWMA	O	50	0	0	0	50
	RB	50	0	0	0	50
	RBAR	50	0	0	0	50

O: the original control chart for the AR(1) model; RB: the original risk-based control chart for independent measurements; and RBAR: the proposed risk-based control chart for the AR(1) model.

In this practical data example, the suggested RBAR design outperformed the competing charts, even though both the risk-based (RB and RBAR) control charts were able to minimize the number of type I mistakes by extending the control region (as seen by the increase in the coefficient k_s), as is obvious from Table 9. In addition, the overall cost of obtaining the decision decreased in both optimized schemes. The EWMA $\bar{X}$ chart was more capable of reducing type I errors in the presence of autocorrelation in the data than the Shewhart $\bar{X}$ chart was. The reason for this is that the EWMA chart works well for individual observations and assigns greater weights to recent observations while still considering past data.

The RB and RBAR average charts were constructed as shown in Fig. 8, where the black lines represent the 'real' process values, whereas the blue lines correspond to the 'observed' sample statistics. The dashed black lines indicate the control limits derived from the RB chart, whereas the dashed blue lines represent those obtained based on the RBAR chart. Instances of incorrect rejections are highlighted with red dots.

The RB design control limits yielded a false alarm at sample number 32 when we assumed independence and ignored the autocorrelation $\phi = 0.178$. However, the proposed RBAR technique removed the type 1 error by incorporating autocorrelation (although minor) into the control limit calculation. Moreover, the results of the proposed RBAR design for the $\bar{X}$ chart were the same as those of the chart proposed by Katona et al. [22] when $\phi = 0$.

Thus, the proposed RBAR charts are more generalized and closer to the real picture of the underlying process.

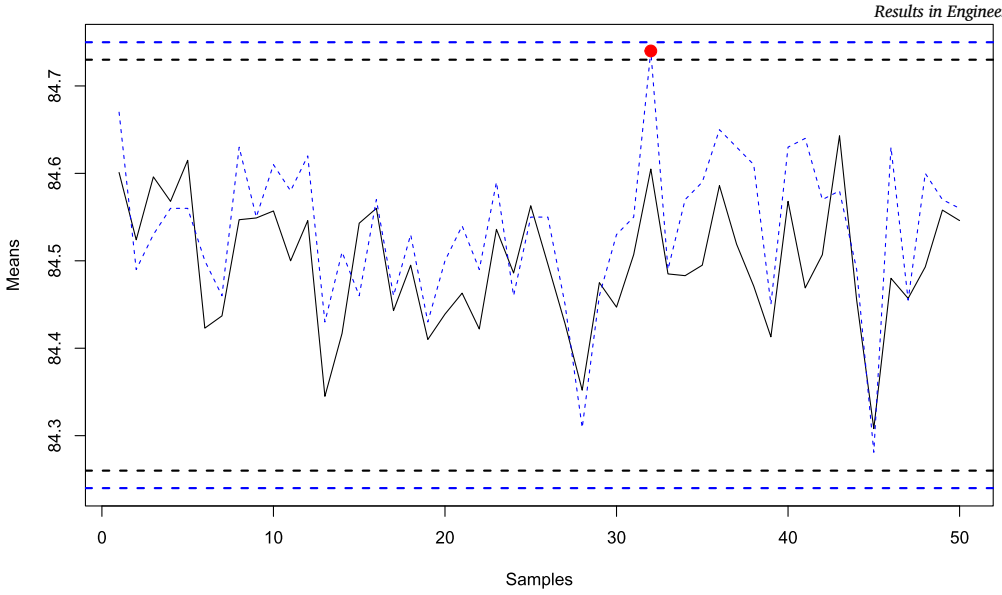

Fig. 8. $\bar{X}$ Control charts produced based on the RB and RBAR schemes for practical data.

4. Summary and conclusion

A major concern in a paradigm that is becoming increasingly industrialized is measurement accuracy. When judgments are being made, it is critical to identify and consider measurement uncertainty. As a result, it is critical to develop process control approaches that consider measurement uncertainty and decision consequences. Autocorrelation is another phenomenon in which the features of interest are dependent. Because various processes conducted in real-world settings result in autocorrelated observations, practitioners are greatly concerned about the considerable degradation exhibited by the detection capabilities of classic control charts when autocorrelation is present. This work advances the field of SQC by integrating RB principles into the control chart design procedure, offering a more holistic view of process monitoring in the presence of autocorrelation and MUs. The primary objective of this study was to suggest a novel design structure for the most widely used memoryless ($\bar{X}$) and memory-based (EWMA) average control charts that can (i) manage dependent observations and (ii) consider the measurement uncertainty and decision outcomes of the target system. Three objectives were sought and accomplished to accomplish this goal.

A more generalized design framework for the RB $\bar{X}$ and RBEWMA $\bar{X}$ control charts was introduced to address scenarios where the assumption of independence among the given observations is violated, particularly in the presence of measurement uncertainty (A_1). This extension is essential for demonstrating that RB average charts are robust not only in cases involving independent samples, as originally validated by Katona [21] but also in processes where the data exhibit autocorrelations. The proposed framework ensures that such charts remain effective in process monitoring tasks under more realistic industrial conditions. When the costs associated with decision errors, such as incorrect acceptances and incorrect rejections, are quantified or at least expressed in relative terms, the overall cost can be considerably decreased (A_2). This holds true for both memory-based and memoryless control charts, even in the presence of autocorrelation, highlighting the importance of integrating cost considerations into the chart design process. The applicability of the proposed method includes not only simulated situations but also actual situations (A_2). Therefore, the proposed generalized design was validated via a simulation and an actual industrial dataset.

The following is a summary of the contributions of this paper. First, the RBCC framework was extended to accommodate autocorrelated measurements, enhancing its applicability in current SPC practices (C_1). This provides a new direction for achieving further enhancements in software development, as these charts are widely used and easily implemented via the rbcc R package. Second, it was shown that RB charts can greatly reduce the total costs of decisions, thus guiding manufacturers who use univariate processes and fixed sample sizes in practice. This can help them lower both the risks and overall costs of their processes with measurement errors, even in the presence of autocorrelation (C_2). Third, the requirement for practically implementing the suggested approach (C_3) is supported by the validation of the suggested generalized RB designs on an actual dataset. The results reveal that the risk-based control charts minimize the overall decision cost of the process by incorporating the cost of each decision in the design. Thus, the proposed charts provide robust tools for practitioners to prioritize interventions on the basis of risk, enhancing decision-making procedures in environments where safety, compliance, and cost efficiency are critical.

5. Limitations and future works

We have demonstrated the effectiveness of the proposed RBAR control charts in terms of handling autocorrelated processes and measurement error scenarios through both simulation studies and real-world data analysis. In this work, we consider AR(1) exclusively because of its simplicity and interpretability of results; it is efficient for short-memory processes and performs reasonably well with smaller datasets. However, certain practical limitations remain.

- The performance of these charts depends on correctly identifying the underlying AR(1) process. Mis-specifying the AR model can lead to biased residuals, impacting both the accuracy of the control limits and the risk estimation results. Practitioners may lack the statistical tools or knowledge that are needed to validate the model assumptions.
- AR-based methods often assume stationarity (constant means and variances over time). Many real-world processes may exhibit nonstationary behaviors, trends, or seasonality, which can distort the performance of these charts.
- Combining autoregressive filtering with RB weighting increases the complexity of data preprocessing (e.g., obtaining the cost vector and estimating the AR coefficients), chart construction (e.g., the overall cost and the observed statistics) and interpretation for practitioners. This may limit the adoption of these methods in industries with limited technical resources or where real-time monitoring is critical.

- The effectiveness of the proposed RBAR charts depends on properly defined risk metrics (e.g., severity × probability), access to reliable historical error data, and a valid cost vector, which may be uncertain or subjective. Misestimated risk weights can lead to misprioritized alarms or delayed responses.
- The charts may perform well for AR(1) processes but could degrade under more complex autocorrelation conditions (e.g., the autoregressive moving average (ARMA) and seasonal ARIMA). Custom tuning might be needed for each process, limiting the general applicability of the developed method.

Future work can extend the RBAR framework to accommodate more complex autocorrelation patterns, such as ARMA or ARIMA models, improving its applicability in nonstationary or seasonally varying environments. The proposed method can easily be extended and implemented using more complex higher order or seasonal processes to predict long-memory prediction/dependency. In this case, large Phase I industrial datasets are needed. Another promising direction is to generalize RBAR charts to multivariate settings, enabling the simultaneous monitoring of interrelated process variables within a unified RB framework. The incorporation of adaptive mechanisms into RBAR charts could enhance their performance in dynamic environments, enabling real-time parameter updates.

CRediT authorship contribution statement

Aamir Saghir: Writing – original draft, Methodology, Investigation, Formal analysis, Data curation, Conceptualization. **Zahid Khan:** Writing – original draft, Software, Methodology, Formal analysis, Data curation, Conceptualization. **Jean-Claude Malela-Majika:** Writing – original draft, Validation, Methodology, Conceptualization. **Zsolt T. Kosztyán:** Writing – original draft, Validation, Supervision.

Computational code availability

The R code used in this study is available from the corresponding author upon request and is ready for direct application by practitioners and researchers.

Declaration of competing interest

The authors declare that they have no known competing financial interests or personal relationships that could have appeared to influence the work reported in this paper.

Acknowledgements

This work was implemented by the TKP2021-NVA-10 project with support provided by the Ministry of Culture and Innovation of Hungary from the National Research, Development and Innovation Fund, financed under the 2021 Thematic Excellence Programme funding scheme.

Data availability

Data sharing does not apply to this article, as no new data were created or analyzed in this study. The real dataset is publicly available in the ***rbcc*** R package under the name *t2uc* (https://CRAN.R-project.org/package=rbcc).

References

[1] V. Alevizakos, K. Chatterjee, C. Koukouvinos, On the performance and comparison of various memory-type control charts, Commun. Stat., Simul. Comput. (2024) 1–21.
[2] B. Aytacoglu, H.S. Sazak, A robust control chart for monitoring the mean of an autocorrelated process, Commun. Stat., Simul. Comput. 44 (2015) 1787–1800.
[3] C.A. Bennett, Effect of measurement error on chemical process control, Ind. Qual. Control 10 (1954) 17–20.
[4] C.M. Borror, D.C. Montgomery, G.C. Runger, Robustness of the ewma control chart to non-normality, J. Qual. Technol. 31 (1999) 309–316.
[5] E.E. Broday, The evolution of quality: from inspection to quality 4.0, Int. J. Qual. Serv. Sci. 14 (2022) 368–382.
[6] I.W. Burr, Statistical Quality Control Methods, Routledge, 2018.
[7] C. Vera do Carmo, L.F.D. Lopes, A.M. Souza, Comparative study of the performance of the cusum and ewma control charts, Comput. Ind. Eng. 46 (2004) 707–724.
[8] C. Chatfield, H. Xing, The Analysis of Time Series: an Introduction with R, Chapman and Hall/CRC, 2019.
[9] F.A.E. Claro, A.F.B. Costa, M.A.G. Machado, Gráficos de controle de ewma e de para monitoramento de processos autocorrelacionados, Produção, 2007.
[10] A.F. Costa, P. Castagliola, Effect of measurement error and autocorrelation on the x chart, J. Appl. Stat. 38 (2011) 661–673.
[11] J. Durbin, G.S. Watson, Testing for serial correlation in least squares regression. iii, Biometrika 58 (1971) 1–19.
[12] C.A. Escobar, J.A. Cantoral-Ceballos, R. Morales-Menendez, Quality 4.0: learning quality control, the evolution of sqc/spc, Qual. Eng. 37 (2025) 92–117.
[13] V. Golosnoy, B. Hildebrandt, S. Köhler, W. Schmid, M.I. Seifert, Control charts for measurement error models, AStA Adv. Stat. Anal. 107 (2023) 693–712.
[14] D.N. Gujarati, D.C. Porter, Basic Econometrics, McGraw-Hill, 2009.
[15] Z. Haizhen, M.B. Khoo, O.T. Babatunde, S. Saha, Effects of measurement errors on semicircle control chart, Qual. Eng. (2024) 1–16.
[16] S. Haridy, A. Maged, N. Alherimi, M. Shamsuzzaman, S. Al-Ali, Optimization design of control charts: a systematic review, Qual. Reliab. Eng. Int. 40 (2024) 2122–2157.
[17] J.J. Horng Shiau, H. Ya-Chen, Robustness of the ewma control chart to non-normality for autocorrelated processes, Qual. Technol. Quant. Manag. 2 (2005) 125–146.
[18] S. Jafarian-Namin, P. Fattahi, A. Salmasnia, Assessing the economic-statistical performance of variable acceptance sampling plans based on loss function, Comput. Stat. (2024) 1–49.
[19] S. Jafarian-Namin, F. Nezhad, R. Tavakkoli-Moghaddam, A. Salmasnia, M. Abooie, An integrated model for optimal selection of quality, maintenance, and production parameters with autocorrelated data, Sci. Iran. 31 (2024) 206–227.
[20] J.E. Jarrett, X. Pan, The quality control chart for monitoring multivariate autocorrelated processes, Comput. Stat. Data Anal. 51 (2007) 3862–3870.
[21] A. Katona, Validation of risk-based quality control techniques: a case study from the automotive industry, J. Appl. Stat. (2021) 1–20.
[22] A.I. Katona, A. Saghir, C. Hegedűs, Z.T. Kosztyán, Design of risk-based univariate control charts with measurement uncertainty, IEEE Access 11 (2023) 97567–97573.
[23] Z. Khan, Smart decision for nanosensor industry using control chart approach, in: Smart Nanosensors, Springer, 2025, pp. 365–383.
[24] Z.T. Kosztyán, T. Csizmadia, C. Hegedűs, Z. Kovács, Treating measurement uncertainty in complete conformity control system, in: Innovations and Advances in Computer Sciences and Engineering, Springer, 2010, pp. 79–84.
[25] Z.T. Kosztyán, C. Hegedűs, A. Katona, Treating measurement uncertainty in industrial conformity control, Cent. Eur. J. Oper. Res. 25 (2017) 907–928.
[26] Z.T. Kosztyán, A.I. Katona, Risk-based multivariate control chart, Expert Syst. Appl. 62 (2016) 250–262.
[27] Z.T. Kosztyán, A.I. Katona, Risk-based x-bar chart with variable sample size and sampling interval, Comput. Ind. Eng. 120 (2018) 308–319.
[28] K.W. Linna, W.H. Woodall, Effect of measurement error on Shewhart control charts, J. Qual. Technol. 33 (2001) 213–222.
[29] B.L. MacCarthy, T. Wasusri, Statistical process control for monitoring scheduling performance—addressing the problem of correlated data, J. Oper. Res. Soc. 52 (2001) 810–820.
[30] M.R. Maleki, A. Amiri, P. Castagliola, Measurement errors in statistical process monitoring: a literature review, Comput. Ind. Eng. 103 (2017) 316–329.
[31] M. Malindzakova, K. Čulková, J. Trpčevská, Shewhart control charts implementation for quality and production management, Processes 11 (2023) 1246.
[32] H.D. Maragah, W.H. Woodall, The effect of autocorrelation on the retrospective x-chart, J. Stat. Comput. Simul. 40 (1992) 29–42.
[33] D.C. Montgomery, Introduction to Statistical Quality Control, John Wiley & Sons, 2020.
[34] T. Munir, X. Hu, O. Kauppila, B. Bergquist, Effect of measurement uncertainty on combined quality control charts, Comput. Ind. Eng. 175 (2023) 108900.
[35] S. Nazari, F. Sogandi, Automated identification of autocorrelated control chart patterns utilizing developed convolutional neural networks, J. Appl. Stat. (2025) 1–19.
[36] H.D. Nguyen, A.A. Nadi, K.D. Tran, P. Castagliola, G. Celano, K.P. Tran, The Shewhart-type rz control chart for monitoring the ratio of autocorrelated variables, Int. J. Prod. Res. 61 (2023) 6746–6771.
[37] H.D. Nguyen, K.P. Tran, G. Celano, P.E. Maravelakis, P. Castagliola, On the effect of the measurement error on Shewhart t and ewma t control charts, Int. J. Adv. Manuf. Technol. 107 (2020) 4317–4332.
[38] A. Papavasileiou, G. Michalos, S. Makris, Quality control in manufacturing–review and challenges on robotic applications, Int. J. Comput. Integr. Manuf. 38 (2025) 79–115.
[39] D. Prajapati, S. Singh, Control charts for monitoring the autocorrelated process parameters: a literature review, Int. J. Product. Qual. Manag. 10 (2012) 207–249.
[40] S. Psarakis, G. Papaleonida, Spc procedures for monitoring autocorrelated processes, Qual. Technol. Quant. Manag. 4 (2007) 501–540.

[41] C. Quintero-Arteaga, R. Peñabaena-Niebles, J.I. Vélez, M. Jubiz-Diaz, Statistical design of an adaptive synthetic x-bar control chart for autocorrelated processes, Qual. Reliab. Eng. Int. 38 (2022) 2475–2500.
[42] A. Roy, D. Cutright, M. Gopalakrishnan, A.B. Yeh, B.B. Mittal, A risk-adjusted control chart to evaluate intensity modulated radiation therapy plan quality, Adv. Radiat. Oncol. 5 (2020) 1032–1041.
[43] H. Sabahno, An adaptive max-type multivariate control chart by considering measurement errors and autocorrelation, J. Stat. Comput. Simul. 93 (2023) 2956–2981.
[44] H. Sabahno, A. Amiri, P. Castagliola, Performance of the variable parameters x control chart in presence of measurement errors, J. Test. Eval. 47 (2019) 480–497.
[45] S. Saha, M.B. Khoo, O.T. Babatunde, S.Y. Teh, W.L. Teoh, Run sum Hotelling's t2 chart for autocorrelated processes, Qual. Reliab. Eng. Int. (2005).
[46] N.A. Saleh, M.A. Mahmoud, L.A. Jones-Farmer, I. Zwetsloot, W.H. Woodall, Another look at the ewma control chart with estimated parameters, J. Qual. Technol. 47 (2015) 363–382.
[47] E. Schat, F. Tuerlinckx, A.C. Smit, B. De Ketelaere, E. Ceulemans, Detecting mean changes in experience sampling data in real time: a comparison of univariate and multivariate statistical process control methods, Psychol. Methods 28 (2023) 1335.
[48] W. Schmid, On the run length of a Shewhart chart for correlated data, Stat. Pap. 36 (1995) 111–130.
[49] W.T. Sheu, S.H. Lu, Y.L. Hsu, The generally weighted moving average control chart for monitoring the process mean of autocorrelated observations, Ann. Oper. Res. (2023) 1–29.
[50] M. Shojaee, S. Noori, S. Jafarian-Namin, F. Hassanvand, A. Johannssen, Designing economic-statistical Hotelling's t 2 control charts for monitoring linear profiles under uncertainty of parameters, J. Stat. Comput. Simul. 94 (2024) 4019–4036.
[51] K. Silpakob, Y. Areepong, S. Sukparungsee, R. Sunthornwat, A new modified ewma control chart for monitoring processes involving autocorrelated data, Intell. Autom. Soft Comput. 36 (2023) 281–298.
[52] T. Smajdorová, D. Noskievičová, Analysis and application of selected control charts suitable for smart manufacturing processes, Appl. Sci. 12 (2022) 5410.
[53] S.H. Steiner, R.J. Cook, V.T. Farewell, T. Treasure, Monitoring surgical performance using risk-adjusted cumulative sum charts, Biostatistics 1 (2000) 441–452.
[54] Z.G.B. Stoumbos, M.R. Reynolds Jr, Robustness to non-normality and autocorrelation of individuals control charts, J. Stat. Comput. Simul. 66 (2000) 145–187.
[55] P.H. Tran, K.P. Tran, A. Rakitzis, A synthetic median control chart for monitoring the process mean with measurement errors, Qual. Reliab. Eng. Int. 35 (2019) 1100–1116.
[56] D. Tyagi, V. Yadav, Combined quality control scheme for monitoring autocorrelated process, Thail. Stat. 22 (2024) 986–1005.
[57] V. Vommi, Murty, S. Seetala, A simple approach for robust economic design of control charts, Comput. Oper. Res. 34 (2007) 2001–2009, https://doi.org/10.1016/j.cor.2005.06.023.
[58] Z. Wang, Y. Li, Construction and application of aewma control chart for autocorrelation process, in: Proceedings of the 2024 4th International Conference on Computational Modeling, Simulation and Data Analysis, 2024, pp. 449–456.
[59] Z. Wu, Asymmetric control limits of the x-bar chart for skewed process distributions, Int. J. Qual. Reliab. Manag. (1996).
[60] A. Yeganeh, A. Johannssen, N. Chukhrova, S.A. Abbasi, F. Pourpanah, Employing machine learning techniques in monitoring autocorrelated profiles, Neural Comput. Appl. 35 (2023) 16321–16340.
[61] N.F. Zhang, Statistical control charts for monitoring the mean of a stationary process, J. Stat. Comput. Simul. 66 (2000) 249–258.
[62] I.M. Zwetsloot, L.A. Jones-Farmer, W.H. Woodall, Monitoring univariate processes using control charts: some practical issues and advice, Qual. Eng. 36 (2024) 487–499.